$$x = \frac{H^o - h_l}{h_{lg}} - \frac{G^2}{2g_c J h_{lg}} \left[ \frac{x v_g}{k} + (1-x) v_l \right]^2 [1 + x(k^2 - 1)] \qquad \text{(A-12)}$$

This is a cubic equation in $x$, and a close first approximation for its trial and error solution is calculated by setting $k = 1$ to obtain the homogeneous quality

$$x^o = \frac{H^o - h_l}{h_{lg}} - \frac{G^2 v_g^2 x^{o2}}{2g_c J h_{lg}} \qquad \text{(A-13)}$$

*Manuscript received September 14, 1964; revision received July 10, 1965; paper accepted July 26, 1965.*

# Heat Transfer to Evaporating Refrigerants in Two-Phase Flow

**J. GERARD LAVIN and EDWIN H. YOUNG**

**The University of Michigan, Ann Arbor, Michigan**

**Flow regimes occurring during evaporation of Freon-12 (dichlorodifluoromethane) and Freon-22 (monochlorodifluoromethane) inside five tubes were investigated. Two flow models are proposed, one each for vertical and horizontal tube orientation. The limits of each flow regime were determined and heat transfer correlations obtained. The most significant flow regimes were found to be nucleate boiling, annular flow, and mist flow. A correlation for the transition between annular flow and mist flow was obtained.**

In previous investigations of heat transfer to refrigerants evaporating inside tubes, the greatest emphasis has been placed on obtaining bulk or overall coefficients for the complete evaporation process. There is a dearth of published information on "point" or local coefficients.

In recent years extensive studies have been made on two-phase flow, and the mechanisms involved have been more clearly defined and described. Several flow regimes have been identified and are thought to be of importance in the evaporation process. Virtually all the work reported in the literature has been carried out with fluids having physical characteristics very different from those of fluorinated hydrocarbon refrigerants, but some of the experimental data are relevant to the problem under consideration here.

The principal purposes of this investigation were to identify the important flow regimes occurring in plain tubes and tubes with internal turbulators, and to study the local heat transfer characteristics of these regimes. One plain tube and four internal fin tubes were used, and details of these are given in Figure 1 and Table 1. Both horizontal and vertical tube orientations were studied, and the working fluids were Freon-12 and Freon-22.

## APPARATUS

Several basic design criteria were established for the design of the apparatus. The first of these was that the vapor-liquid mixture fed to the test section was obtained by generating and mixing two streams, one of slightly subcooled liquid and the other of superheated vapor, each stream being metered separately. Heat was generated within the walls of the test section by electrical (d.c.) resistance heating. The test section was sufficiently short to keep pressure, temperature, and vapor fraction essentially constant along it. Test section units were easily removable, since a number of them were used, and provision was made to rotate the test section from the horizontal to the vertical position.

A diagram of the apparatus is shown in Figure 2. Starting from the receiver, liquid was fed to the pump, passing through a filter-drier en route. The liquid stream leaving the pump was split into two parts, one going to the evaporator and the other to a metering section. Superheated vapor was generated in the

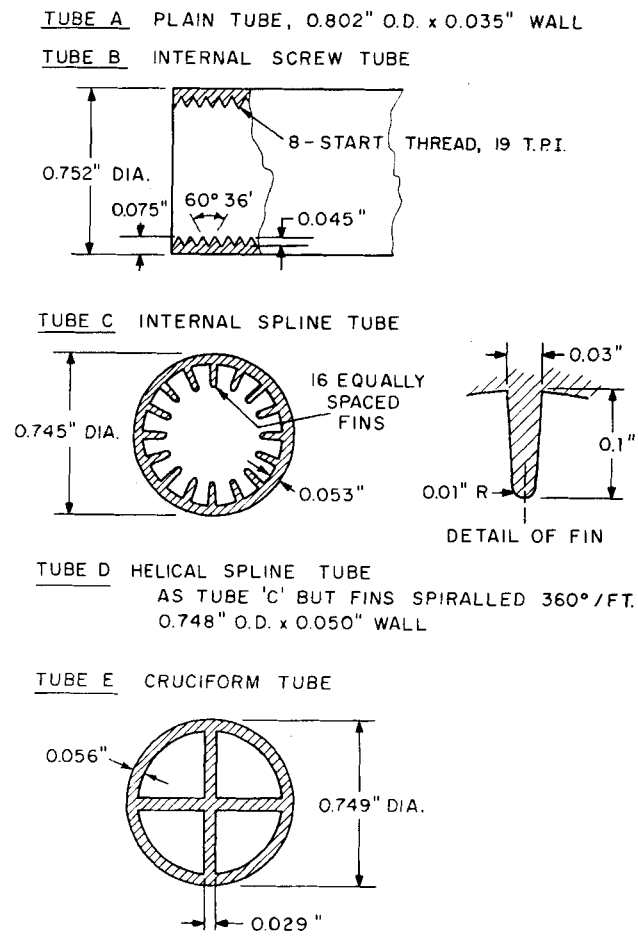


**Fig. 1. Details of tubes.**

J. G. Lavin is with E. I. duPont deNemours and Company, Inc., Wilmington, Delaware.

evaporator and fed to a metering section, where temperature, pressure, and flow rates were measured. Both streams entered a mixing section and then passed to the section through a flexible steel tube. The mixture leaving the test section was fed into the condenser, from which subcooled condensate passed to the receiver.

On arrival at the test section, fluid first passed through a sight section and then an 18-in. calming length. Next came the electrically heated test section. Two copper electrodes, 6 in. sq., were silver soldered onto the tube, 12 in. apart. Pressure taps were inserted at the electrodes. The electrodes were connected to the laboratory bus-bar system by flexible copper cables. Wall temperatures were measured at the midpoint of the heated length by copper-constantan thermocouples clamped to the tube and insulated from it by a strip of mica 0.0015 in. thick. The heated length was followed by an 18 in. length of tube and another sight section. Safety features included a thermocouple relay switch located close to the end of the heated length, which cut off the current to the test section when the temperature rose above 600°F. and air-operated, quick-acting valves located at each end of the test section.

## MEASUREMENTS

Flow rates of vapor and of liquid were metered by measurement of pressure drop across calibrated orifices with mercury manometers. Temperatures were measured with calibrated thermocouples and pressures by calibrated bourdon tube gauges. Accuracy of these instruments was frequently checked by comparing test section wall temperatures with the saturation temperature corresponding to the test-section inlet pressure, under conditions of zero heat input and low flow rate of vapor-liquid mixture through the test section.

## FLOW REGIMES

Recent publications (*1* to 3) have shown that the flow regimes occurring in two-phase systems with the addition of heat are different from those occurring without the addition of heat. Two models are proposed for the evaporation process, one for the vertical and one for the horizontal tube orientation. Diagrams are shown on Figures 3 and 4. These models are based on visual observations reported in the literature and visual observations made during this investigation.

In the case of the vertical tube, liquid subcooled below its saturation temperature enters the tube and nucleate boiling begins when the tube wall reaches a temperature exceeding the saturation temperature by a small amount. Bubbles detach from the wall and collapse in the central core of the liquid. When the bulk temperature approaches saturation, bubbles tend to coagulate and form slugs which later break down to form an annular flow. This transition was observed by Sachs and Long (3) to occur at 1% vapor quality (quality being defined here as the percentage of total mass flow in the form of vapor), and examination of the data of other investigators (*4*, 5) indicates that the transition is normally completed between 1 and 2% quality.

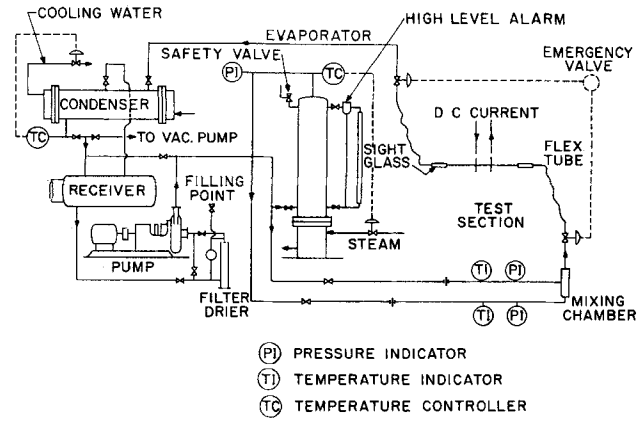


**Fig. 2. Diagram of apparatus.**

As the vapor quality increases, slip flow develops between the two phases and small droplets of liquid are picked up from the interface by the high velocity vapor stream. A large population of droplets forms in the central core continuously migrating to the liquid stream. This is the annular mist regime.

When the vapor quality reaches a certain critical value, the amount of liquid present becomes insufficient to maintain a stable film on the walls. This is the condition sometimes referred to as two-phase burnout or dry wall condition. However, recent investigations (*6*, *7*) have shown that the transition occurs over a region rather than at a point. In this paper, the term *upper transition region* will be used to identify this phenomenon.

After the transition region there is a change over to a mist flow regime in which the walls are dry and the mechanisms of heat transfer are those of forced convection to a gas stream with migration of droplets to the wall with vaporization on contact. Small droplets have been observed to exist even in superheated vapor (*7*, *8*).

The mechanisms occurring in the horizontal tube case are only slightly different from those occurring in the vertical tube case. The first important difference observed is that, instead of forming slugs, bubbles tend to rise to the top of the tube cross section. Stratified flow with nucleate boiling ensues. This continues until the vapor velocity becomes sufficiently high to support an annular flow regime. In stratified flow, the upper walls are wetted by the wave crests of the free surface and capillary forces. In the annular flow regime, gravitational forces act upon the liquid film and tend to make the film at the top of the tube somewhat thinner than the film at the bottom of the tube (9). Once annular flow develops, the process becomes the same as in the vertical case.

## RESULTS AND DISCUSSION

Since the test section was heated by generating heat within the walls of the test section itself, and temperature

TABLE 1. DETAILS OF TUBES

| Tube | Description | External surface area, sq. ft./ft. | Internal surface area, sq. ft./ft. | Unobstructed flow area, sq. ft. | Equivalent diameter, ft. | Inside/outside area ratio | Construction material |
|---|---|---|---|---|---|---|---|
| *A* | Plain | 0.210 | 0.191 | 0.00293 | 0.0608 | 0.912 | Copper |
| *B* | Internal screw | 0.197 | 0.339 | 0.00197 | 0.0271 | 1.722 | Copper |
| *C* | Internal longitudinal fin | 0.195 | 0.409 | 0.00196 | 0.0191 | 2.095 | Copper |
| *D* | Internal longitudinal spiral fin | 0.196 | 0.414 | 0.00202 | 0.0196 | 2.110 | Copper |
| *E* | Cruciform | 0.196 | 0.342 | 0.00174 | 0.0206 | 1.745 | Aluminum |

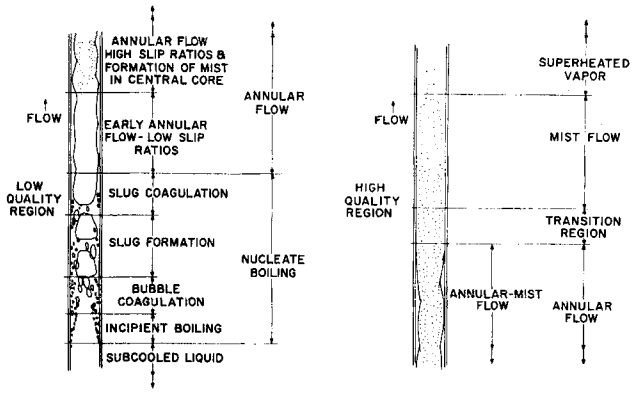


**Fig. 3. Model of process of evaporation inside a vertical tube.**

measurements were made on the outside wall of the tube, it was necessary to compute the temperature drop across the wall. This was obtained from the equation for conduction with internal heat generation in a cylindrical geometry. Since the tubes were made of copper or aluminum, the temperature drop was found to be negligibly small in all cases and was therefore disregarded. Fin efficiencies were examined and were found to be very close to 100% in all cases.

Experimental heat transfer coefficients were obtained from Equation (1)

$$h = \frac{(q/A)}{T_w - T_{sat}} \tag{1}$$

where $A$ was based on the total internal tube surface. In the case of the finned tubes, the area was prime surface plus fin surface area. Physical properties were evaluated at saturation temperatures unless otherwise stated.

The experimental fluids were Freon-12 and Freon-22. Saturation temperatures varied between 75° and 100°F., mass flow rates between 400,000 and 2,300,000 lb./(hr.) (sq. ft.), and heat fluxes between 400 and 12,000 B.t.u./(hr.) (sq. ft.). The range of vapor fractions studied was annular flow regime, 0.17 to 0.89; transition region, 0.63 to 0.99; mist flow regime, 0.64 to 1.0. In the nucleate boiling regime the liquid was slightly subcooled.

## NUCLEATE BOILING REGIME

Experimental nucleate boiling heat transfer data were obtained on the plain tube in both the horizontal and vertical position with Freon-12 and Freon-22. Data were obtained in the finned tubes with Freon-12.

The experimental data were correlated by McNelly's equation (*10*), which had previously been used to correlate the Freon-12 data of Myers and Katz (*11*), and which had also been found useful for a number of organic liquids. The equation used was

$$\frac{h_b D_e}{k_l} = C_1 \left[\frac{Q D_e}{\mu \lambda}\right]^{0.69} \left[\frac{c \mu}{k}\right]^{0.69} \left[\frac{\rho_l}{\rho_v} - 1\right]^{0.31} \left[\frac{p D_e}{\sigma}\right] \tag{2}$$

The value for the constant $C_1$ obtained by McNelly was 0.225. Figure 5 shows a comparison of the experimental Nusselt number with the Nusselt number obtained from Equation (2) with the constant $C_1$ equal to 0.225. The plain tube data show that the heat transfer coefficient is independent of tube orientation and consequently no distinction is made between the vertical and horizontal cases for the finned tube data. All the experimental Nusselt numbers were higher than those predicted by the original McNelly equation. New constants were obtained for each

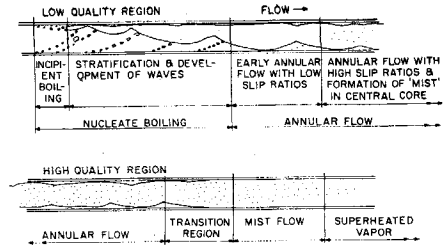


**Fig. 4. Model of process of evaporation inside a horizontal tube.**

tube. Average values for the constant $C_1$ are given in Table 2.

Figure 6 shows the coefficients for the finned tubes, on a square foot of area basis, to be much higher than those for the plain tube. This effect was also noted by Myers and Katz (*11*).The explanation for this may be that the sharp corners found in each of the fin configurations provide conditions favorable to nucleation. The two spline tubes and the internal screw tube had very different internal configurations, but the corner length per foot was about the same in each case. The data for all three tubes were correlated by a single line. The corner length per foot for the cruciform tube was about one-third of that for the other three internal fin tubes, and the correlation line fell about half-way between the plain tube line and the line for the spline and internal screw tubes. The data of this investigation, therefore, appeared to support such an explanation.

## ANNULAR FLOW REGIME

Experimental annular flow heat transfer data were obtained on the plain tube in both the horizontal and vertical positions with Freon-12 and Freon-22. Data were obtained on the finned tubes in both positions with Freon-12.

The form of the equation chosen to correlate the data was

$$\frac{h_{tp}}{h_l}\left[\frac{G\lambda}{Q}\right]^{0.1} = C_2\left[\frac{1+x}{1-x}\right]^{1.16} \tag{3}$$

The heat transfer coefficient for the liquid alone was obtained from the Sieder-Tate equation:

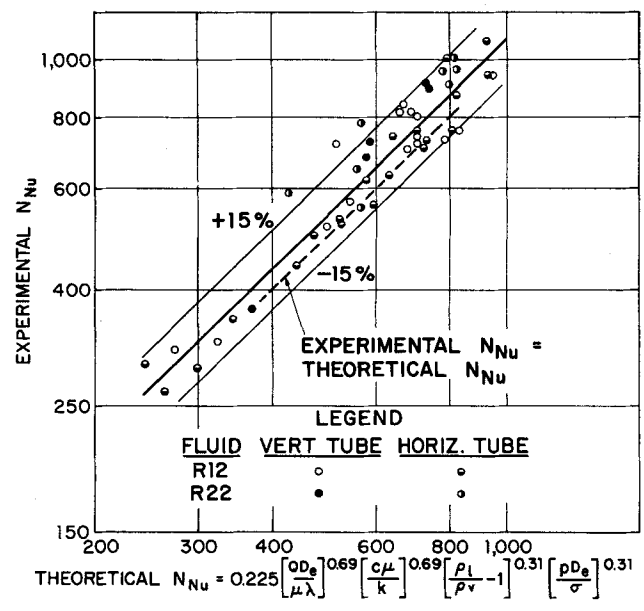


**Fig. 5. Nucleate boiling correlation for plain tube.**

TABLE 2. VALUES OF CONSTANTS IN CORRELATING EQUATIONS

| Tube | $C_1$ | $C_2$ | $C_3$ | $C_4$ | $C_5$ | $C_6$ |
|---|---|---|---|---|---|---|
| $A$ | 0.25 | 3.79[1] | 0.023 | $3.07 \times 10^{-8}$ | 0.0191 | 0.0162 |
| $B$ | 0.5 | 5.04 | 0.0138 | $7.61 \times 10^{-8}$ | — | — |
| $C$ | 0.5 | 5.04 | 0.0167 | $7.61 \times 10^{-8}$ | 0.0138 | 0.0117 |
| $D$ | 0.5 | 5.04 | — | $7.61 \times 10^{-8}$ | — | — |
| $E$ | 0.33 | 3.50 | 0.0097 | $6.54 \times 10^{-8}$ | 0.0121 | 0.01025 |

Note: The value of $C_2$ for tube $A$ is a function of tube orientation. The value for the vertical tube is 3.79 as shown, and the value for the horizontal tube is 6.59. The values shown for other tubes are not a function of orientation.

$$N_{Nu} = C_3 N_{Re}^{0.8} N_{Pr}^{1/3} \left[\frac{\mu}{\mu_w}\right]^{0.14} \tag{4}$$

Following Guerrieri and Talty (5), the Reynolds number was defined as the number obtained if only the liquid fraction was flowing inside the tube.

$$(N_{Re})_l = \frac{G D_e (1-x)}{\mu_l} \tag{5}$$

The constant $C_3$ was set equal to 0.023 and the following equation for $h_l$ was obtained.

$$h_l = 0.023 \frac{k}{D_e}\left[\frac{G D_e (1-x)}{\mu_l}\right]^{0.8}\left[\frac{c\mu}{k}\right]^{1/3}\left[\frac{\mu}{\mu_w}\right]^{0.14} \tag{6}$$

Figure 7 shows a plot of

$$\frac{h_{tp}}{h_l}\left[\frac{G\lambda}{Q}\right]^{0.1} \text{ vs. } \left[\frac{1+x}{1-x}\right]$$

for the plain tube points.

The points for the horizontal tube orientation were significantly higher than those for the vertical and the Freon-22 points were in good agreement with those of Freon-12. The constant $C_2$ in Equation (3) was found by regression analysis on an IBM-7090 digital computer using the Dallemand-General motors program for each tube studied. The values are tabulated in Table 2.

Data obtained on the four finned tubes are shown in correlated form on Figure 8. The data for the internal screw tube and the two spline tubes were in good agreement and were correlated by a single line. Both horizontal and vertical tube data were obtained on the cruciform tube. Although the horizontal tube points appeared to fall slightly higher than the vertical tube points, the difference was not significant, and all the data for this tube were correlated by a single line. The data were correlated by Equation (3), the exponent 1.16 being held at the value obtained for the plain tube and the constant $C_2$ representing an average value for the appropriate data set. The values obtained for the constants for the finned tubes are also listed in Table 2.

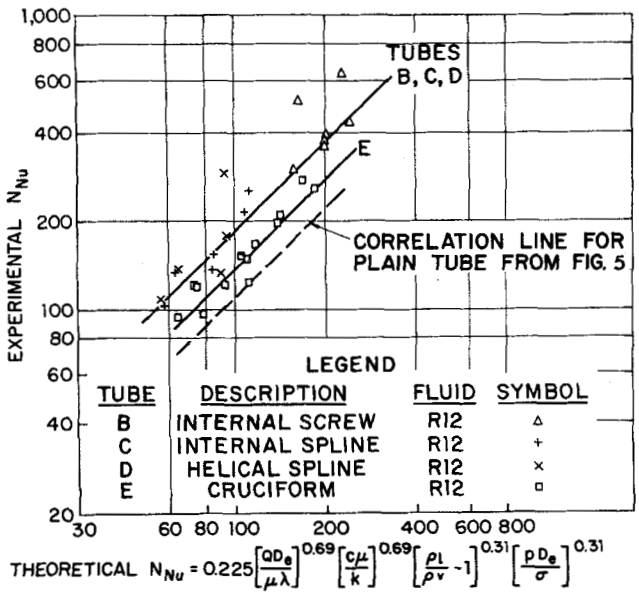


Fig. 6. Nucleate boiling correlation for finned tube.

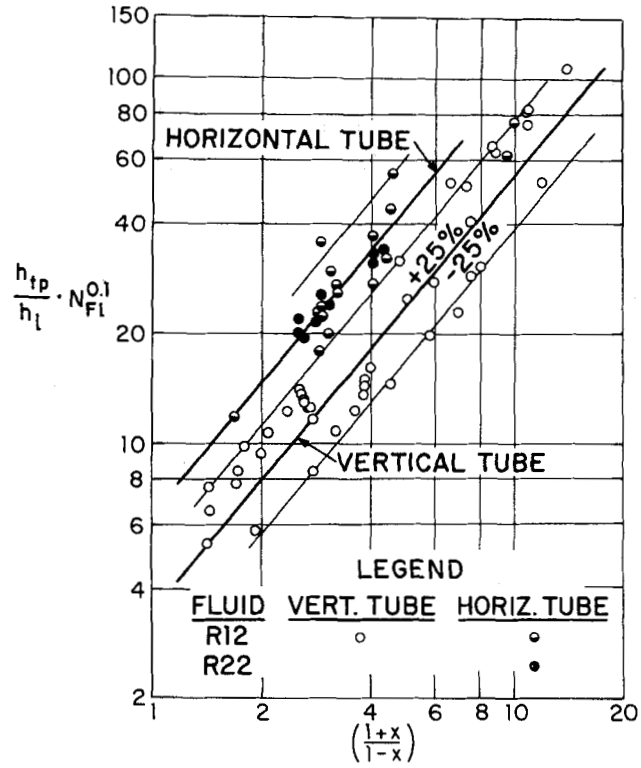


Fig. 7. Annular flow regime, plain tube data.

In order to check the validity of the equations used for predicting $h_l$, experimental data were obtained for heat transfer to subcooled Freon-22 liquid in the plain tube, and the internal screw, spline, and cruciform tubes. Figure 9 shows a plot of the experimental Nusselt number vs. the Nusselt number predicted by Equation (4), with $C_3$ set equal to 0.023. The agreement between the experimental and predicted values in the case of the plain tube was good. The experimental values for the finned tubes, however, were somewhat less than the predicted values. New values for the constant $C_3$ in Equation (4) were obtained for each of the finned tubes, and these are listed in Table 2.

In Figure 7 it will be observed that the horizontal tube points fell significantly higher than the vertical tube points. An explanation of the superior performance of the horizontal tube orientation may be found in an examination of the flow mechanisms involved.

In the vertical tube, bulk transport of the liquid phase took place through helical waves superimposed upon a thin stable film, and the time-mean film thickness was the same all around the tube. In the horizontal tube the liquid tended to fall to the lower part of the tube and the walls were wetted by a combination of three factors: surface tension effects, wave crests, and deposition of droplets from the central vapor core. This resulted in a low mean film thickness over a large part of the tube and led to higher coefficients.

In the finned tube experiments, data were obtained in both horizontal and vertical tube orientations for one tube only, the cruciform tube. In this case there was no significant difference between the two orientations. The vertical tube points for the internal screw, spline, and helical spline tubes were significantly higher than those for the vertical plain tube. The points for the cruciform tube were not significantly different from those for the vertical plain tube. This led to the conclusion that the internal fin configurations, in general, changed the liquid holdup pattern in the tube, giving thinner films than would be expected in a plain tube of the same inside diameter. The cruciform tube, however, simply behaved like four small diameter tubes.

Figure 10 presents a comparison made between some of the data from this study and that from other studies relating to annular flow. In order to make the comparison on the same basis, only the vertical plain tube points were used. The ratio $(h_{tp}/h_l)$ was plotted against the Martinelli factor $(1/X_{tt})$. In this comparison, the heat transfer coefficient for liquid alone $h_l$ was defined as

$$h_l = 0.023 \left[\frac{k}{D_e}\right]\left[\frac{G D_e}{\mu}\right]^{0.8}[N_{Pr}]^{0.4} \qquad (7)$$

It should be noted that the Freon-12 data covered a higher quality range (up to 89%) than the other investigations. Guerrieri and Talty (5) covered up to 11% with five organic liquids and Bennett et al. (*12*) and Dengler and Addoms (*4*) up to 59 and 71%, respectively, each working with water. The range of the Freon-12 data on the $1/X_{tt}$ axis was smaller than the others because of the relatively low value of the group $(\rho_l/\rho_v)$.

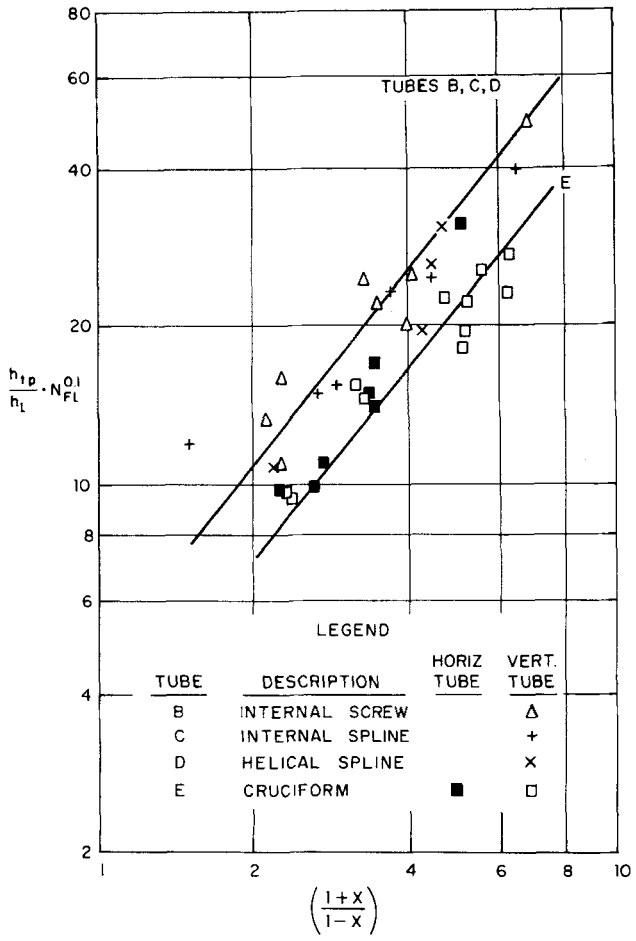


Fig. 8. Annular flow regime, Freon-12, finned tube data.

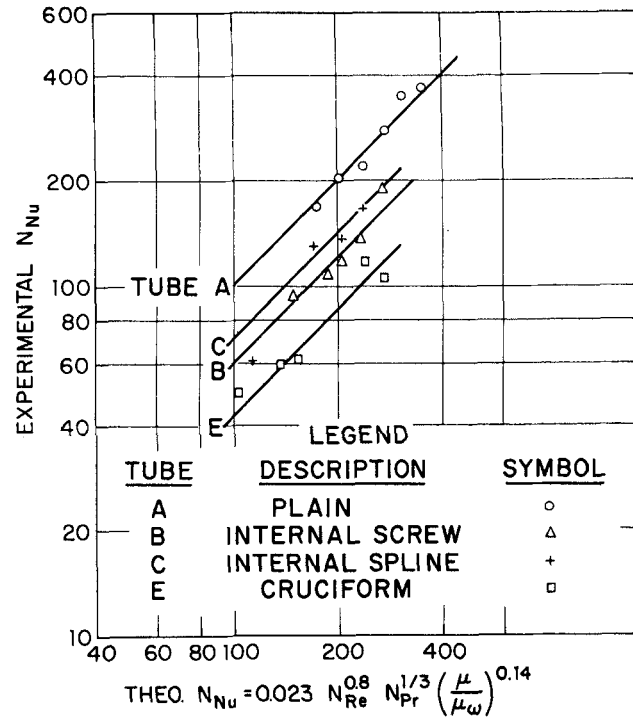


Fig. 9. Subcooled liquid data for Freon-22.

The correlating line for the data of this study was found to fall considerably below the correlation lines of the other investigators. This may be explained as follows.

The correlations of Guerrieri and Talty, Dengler and Addoms, and Bennett et al. were all of the following form:

$$\frac{h_{tp}}{h_l} = C\left[\frac{1}{X_{tt}}\right]^n ; \quad 0.45 < n < 0.72 \qquad (8)$$

where

$$\frac{1}{X_{tt}} = \left[\frac{x}{1-x}\right]^{0.9}\left[\frac{\rho_l}{\rho_v}\right]^{0.5}\left[\frac{\mu_v}{\mu_l}\right]^{0.1} \qquad (9)$$

although Bennett et al. also included a heat flux term in Equation (8).

On examination of the above equations it was found that, for a given vapor fraction

$$h_{tp} = C\left[\frac{\rho_l}{\rho_v}\right]^{0.25} \approx C\left[\frac{v_v}{v_l}\right]^{0.25} \qquad (10)$$

In contrast to this, Groothius and Hendal (*13*), working with two-phase, two-component systems, found the two-phase heat transfer coefficient to be strongly dependent upon the volumetric flow ratio of gas to liquid. This suggested that the Martinelli parameter as defined in Equation (9) did not describe sufficiently well the effect of the vapor-liquid velocity ratio, and hence the vapor-liquid density ratio on the two-phase heat transfer coefficient. Typical values of $(\rho_l/\rho_v)$ for the four experiments are

| | | | |
|---|---|---|---|
| Dengler and Addoms, | $\rho_l/\rho_v$ | between | 300 and 60 |
| Guerrieri and Talty, | $\rho_l/\rho_v$ | between | 420 and 230 |
| Bennett et al., | $\rho_l/\rho_v$ | between | 160 and 30 |
| This investigation, | $\rho_l/\rho_v$ | between | 35 and 20 |

The density ratio for this investigation is at least one order of magnitude less than that of the other investigators. This supports the explanation offered above. If the Martinelli factor is to be extensively used in two-phase heat transfer work, then it would seem that the exponents on the various groups should be evaluated experimentally from heat

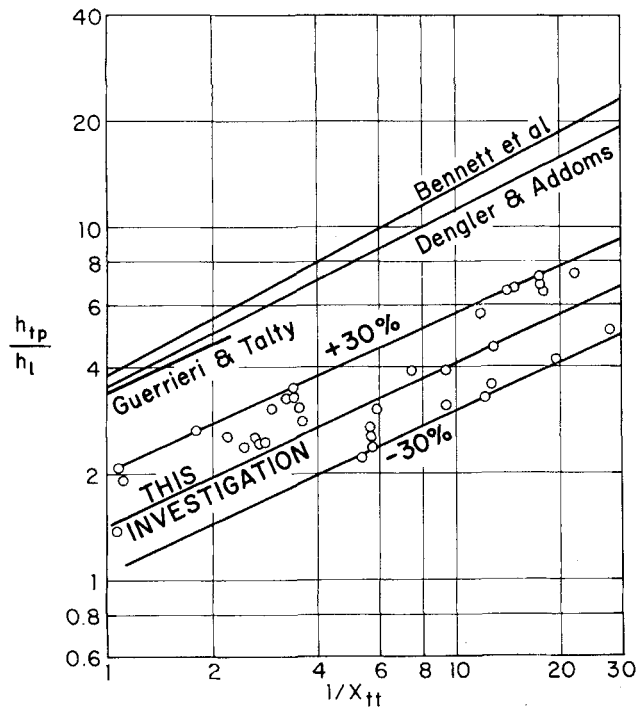


Fig. 10. Comparison of data for vertical plain tube and Freon-12 with that of other workers.

transfer data rather than pressure drop data, which is presently the case.

## TRANSITION BETWEEN ANNULAR FLOW AND MIST FLOW REGIMES

Experimental data for the onset of the upper transition region were obtained on all five tubes. Data were obtained with Freon-12 and Freon-22 for the plain tube in both the horizontal and vertical positions. Finned tube data were obtained with Freon-12 and in the vertical position only, except in the case of the cruciform tube, where data were also obtained in the horizontal position.

It was suggested by Groothius and Hendal (*13*) that the Weber number, properly defined, could be used to characterize the onset of the transition region. Preliminary analysis showed the Weber number to be dependent upon the vapor Reynolds number, the flux number, and the vapor-liquid density ratio. A correlation of the following form was assumed:

$$N_{We} = C_4 (N_{Re})_v^a (N_{Fl})^b \left[\frac{\rho_l}{\rho_v}\right] \qquad (11)$$

The exponent on the density ratio term was arbitrarily set equal to 1.0 because of the small range of variation in these experiments.

The plain tube data for Freon-12 and Freon-22 were subjected to computer regression analysis and the following equation obtained:

$$N_{We} = 3.07 \times 10^{-8} (N_{Re})_v^{1.0} (N_{Fl})^{0.06} \left[\frac{\rho_l}{\rho_v}\right] \qquad (12)$$

The data obtained for finned tubes were then analyzed in a similar way. The exponents on the groups in Equation (10) were used, and an average value of the constant $C_4$ for each of the tubes was obtained and is listed in Table 2.

Figure 11 shows the experimental Weber number plotted against the expression

$$(N_{Re})_v (N_{Fl})^{0.06} \left[\frac{\rho_l}{\rho_v}\right]$$

A simple model permitted the development of correction factors to put the fin tube data on the same basis as the plain tube data. The model was dependent on the assumption that for a given liquid, temperature, and heat flux, the critical factors were vapor velocity, liquid velocity, and liquid film thickness. If transition occurred at certain values of these three parameters in one tube, then it would occur at the same values in any other tube, whatever the shape or size.

As an example, consider a case in which data on the vapor fraction at transition in a 1-in. diameter tube are used to predict the vapor fraction at the onset of transition in a 2-in. diameter tube. Since the vapor velocity is to remain the same and the liquid film on the wall is thin, the weight flow rate of vapor flowing through the new tube will increase in the ratio of the tube areas, or by a factor of 4. Since the liquid velocity and film thickness are also to remain the same, the weight flow rate of liquid in the new tube will increase in the ratio of the circumferences, or by a factor of 2. Thus, it will be seen that the vapor fraction at transition will be much higher in the case of the 2-in. tube than in the case of the 1-in. tube. With this approach, correction factors were developed for $G$, the total mass flow rate and $x$, the vapor fraction. These are given in Equations (13) and (14). Derivations are given in detail in Appendix 6 of reference 7.

$$x_2 = \frac{x_1}{1 + \left[\frac{D_{e,1}}{D_{e,2}} (1 - x_1)\right]} \qquad (13)$$

and

$$G_2 = G_1 \left[x_1 + \frac{D_{e,1}}{D_{e,2}} (1 - x_1)\right] \qquad (14)$$

Application of these correction factors to the Weber number and the Reynolds number leads to the following equations:

$$(N'_{Re})_v = (N_{Re})_{v,1} \left[\frac{D_{e,2}}{D_{e,1}}\right] \qquad (15)$$

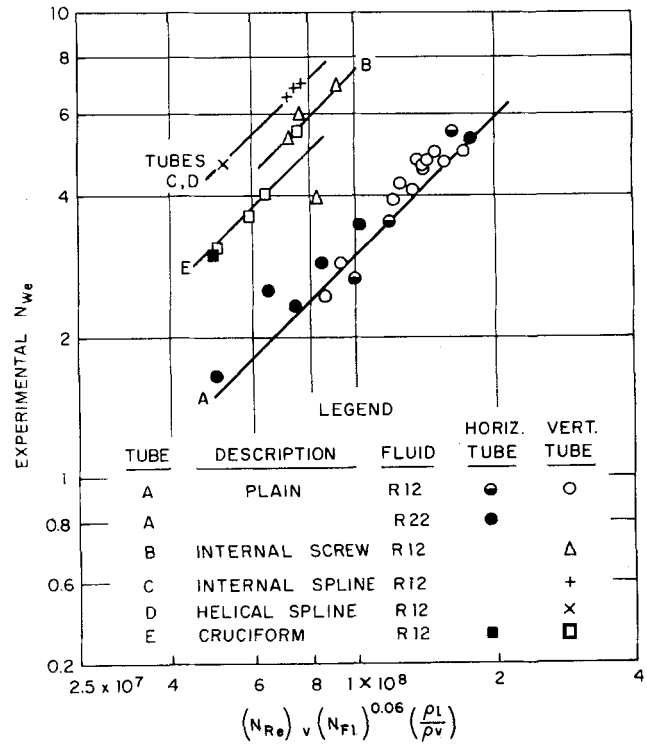


Fig. 11. Upper transition region data for Freons-12 and 22, plain and finned tubes.

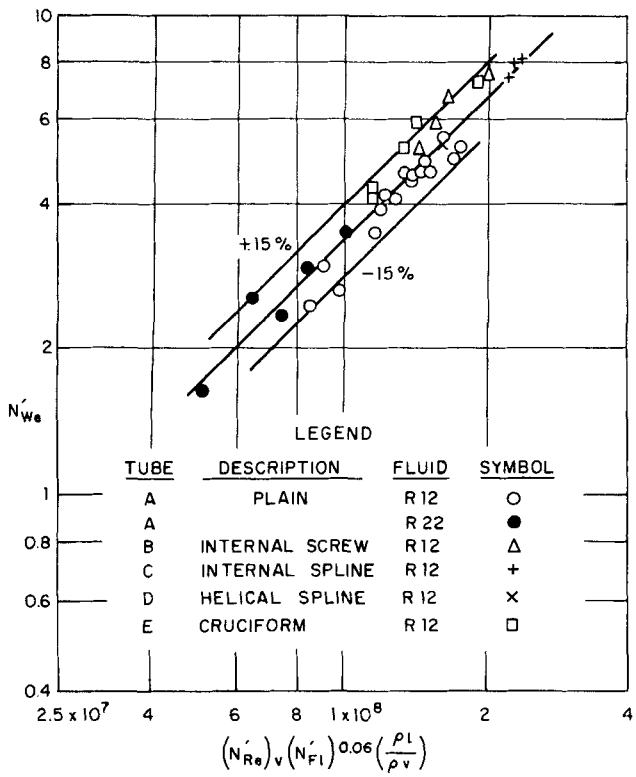


Fig. 12. Upper transition region finned tube data corrected to tube A.

$$N'_{We} = \frac{(N_{We})_1}{x_1 + \left[\frac{D_{e,2}}{D_{e,1}}(1-x_1)\right]} \tag{16}$$

$$N'_{Fl} = \frac{G_l \lambda}{Q}\left[x_1 + \frac{D_{e,1}}{D_{e,2}}(1-x_1)\right] \tag{17}$$

The following equation was obtained to correlate all the data for plain and finned tubes.

$$N'_{We} = 3.07 \times 10^{-8} (N'_{Re})_v (N'_{Fl})^{0.06}\left[\frac{\rho_l}{\rho_v}\right] \tag{18a}$$

and Figure 12 shows the modified experimental Weber number $N'_{We}$ plotted against

$$(N'_{Re})_v (N'_{Fl})^{0.06}\left[\frac{\rho_l}{\rho_v}\right]$$

for all tubes.

With the apparatus used, it was not possible to obtain heat transfer coefficients within the transition region or to study the conditions under which the transition region ends and stable mist flow is established. The only data of this kind presently available are that of Silvestri (6), reproduced in Figure 13. The data presented in Figure 11 show little dependence upon tube orientation, within the area of the correlation. The data points for Freon-22 are in good agreement with those for Freon-12.

Of greatest interest here is the method presented for correlation of the data on different tubes, the results of which are shown in Figure 12. The Freon-12 finned tube data fall within the limits of the plain tube data, indicating the validity of the correlation for a wide range of tube types. It will be noted that the transition between annular flow and mist flow occurs somewhat earlier with finned than with plain tubes. If the transition were normally to take place at, say, 70% quality in the plain tube, then in the case of the internal screw tube it might take place as early as 50%. This is important, since two-phase heat transfer coefficients increase all the way up to burnout, and mist flow coefficients are considerably lower than the annular flow coefficients.

## COMPARISON WITH DATA OF OTHER INVESTIGATORS

Two papers are available in the literature containing data capable of conversion into a form suitable for comparison. Rounthwaite and Clouston (9) presented four data points for water at 200, 400, 500 and 600 lb./sq. in. Silvestri (6) presented fifteen data points for water at approximately 1,000 lb./sq. in. on nine different test sections. These data points, analyzed according to Equation (16), are shown plotted in Figure 14, together with representative refrigerant points from Figure 12. The water data showed good internal consistency but were not in good agreement with the refrigerant data. The two sets of data could be correlated by increasing the value of the exponent on the vapor Reynolds number in Equation (18). However, the validity of such a correlation would have to be substantiated by data at lower Reynolds numbers for the refrigerants, and higher Reynolds numbers for water. It should be noted that the Weber number is strongly dependent upon the value used for surface tension. Consistent high temperature surface tension data for water are not easily obtained, and the interested reader is referred to reference 7 for the values used in this comparison.

Examination of the expanded form of Equation (18a)

$$\frac{x^2 G \mu_l}{g_c \sigma \rho_v}\left[\frac{G D_e}{\mu_l}\right]^{0.125} = C\left[\frac{G D_e x}{\mu_v}\right]\left[\frac{Gx}{Q}\right]^{0.06}\left[\frac{\rho_l}{\rho_v}\right] \tag{18b}$$

shows that for any given fluid the vapor fraction at transition is only weakly dependent upon mass flow rate, heat flux, and physical properties. The most important single factor is the equivalent diameter of the tube.

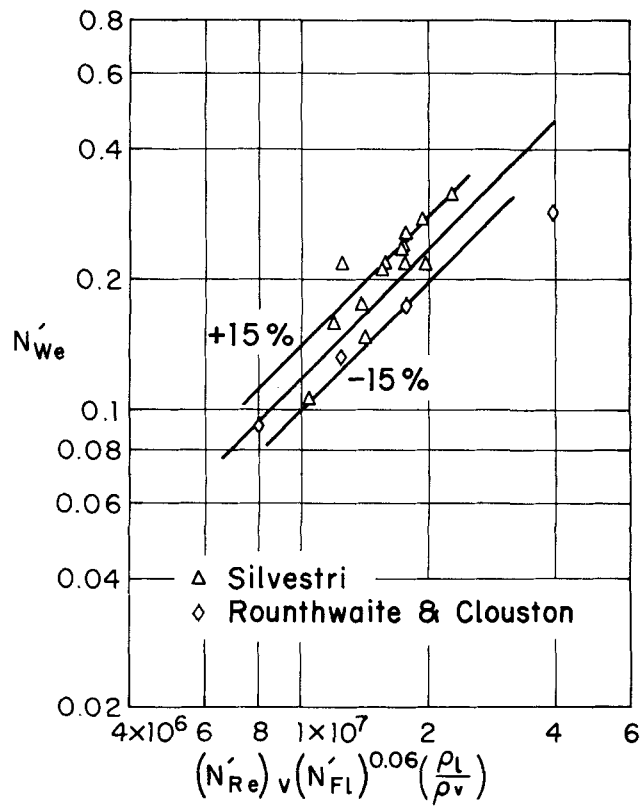


Fig. 13. Upper transition region data for water.

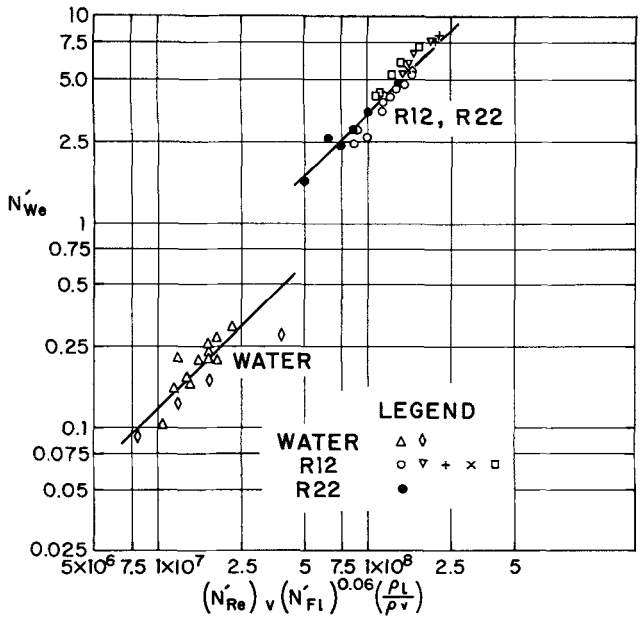


Fig. 14. Upper transition region comparison of Freon and water data.

Correlation lines for tubes of shapes and sizes not covered in this study may be obtained by correcting the data given here with the use of Equations (13) to (18). The limits to which such extrapolations can be made are not yet clear, but certainly moderate changes in size and variations within the classes of fin configurations studied should not present any problem.

## MIST FLOW REGIME

Experimental heat transfer data in the mist flow regime were obtained on Freon-12 and Freon-22 for the plain tube in both horizontal and vertical positions. Data on Freon-12 were obtained for the spline tube in the vertical position and for the cruciform tube in both the horizontal and vertical positions.

The superheated vapor correlations of Heineman (*14*) were chosen as a basis for the mist flow correlations. Heineman's correlations were

$$(N_{Nu})_f = 0.157\,(N_{Re})_f^{0.84}\,(N_{Pr})_f^{1/3}\,(L/D_e)^{-0.04} \quad \text{for } 6 < L/D_e < 60. \tag{19}$$

and

$$(N_{Nu})_f = 0.0133\,(N_{Re})_f^{0.84}\,(N_{Pr})_f^{1/3} \quad \text{for } L/D_e > 60 \tag{20}$$

where physical properties are evaluated at a film temperature, which is taken to be the mean of wall and bulk temperatures. The two forms of the correlating equation were included because experimental measurements were taken at low $L/D_e$ ratios (8 to 23), where entrance effects are still important, but in practice, only the coefficients away from the entrance region are of interest.

The Prandtl number was virtually constant in these experiments, and in order to isolate the effect of liquid droplets present on the coefficient, the value $(N_{Nu})_f/(N_{Re})_{v,f}^{0.84}$ was plotted against $(1 - x)$ for the plain tube data and the following relationship found.

$$[(N_{Nu})_f/(N_{Re})_{v,f}^{0.84}] = C\,(1-x)^{0.1} \tag{21}$$

The $(1 - x)$ term was introduced into Equation (19) which became

$$\left[\frac{h_{tp}\,D_e}{k_v}\right] = C_5 (N_{Re})_{v,f}^{0.84} (N_{Pr})_{v,f}^{1/3} (L/D_e)^{-0.04} (1-x)^{0.1} \tag{22}$$

and the average values for the constant $C_5$ obtained for each data set. These are given in Table 2.

Figure 15 shows the experimental Nusselt number plotted against the Nusselt number predicted from Equation (22) with $C_5 = 0.0157$. Since the values of the constant $C_5$ obtained differed from the Heineman value of 0.0157, it was necessary to obtain new constants $C_6$ for Equation (22). This was done by increasing the value of the constant for each tube in the same proportion as in Equation (17), that is

$$C_6 = C_5\left[\frac{0.0133}{0.0157}\right] \tag{23}$$

which leads to the equation

$$\left[\frac{h_{tp}\,D_e}{k_v}\right]_f = C_6\,(N_{Re})_{v,f}^{0.84}(N_{Pr})_{v,f}^{1/3}(1-x)^{0.1} \tag{24}$$

and where the values of $C_6$ are given in Table 2.

Although several attempts were made to obtain data on the internal screw tube in this regime, none were successful, even at vapor fractions very close to 1.0. A cyclic temperature fluctuation was noted in all cases, and a pronounced tangential component of flow was observed. This suggests that centrifugal forces assist the migration of droplets to the wall and thus bring about the temperature instabilities observed. It would be expected that this would lead to higher coefficients.

Mist flow coefficients were slightly higher than those expected for superheated vapor under the same conditions. This suggests that the Heineman equation (*20*) can be used with confidence for computing superheated vapor coefficients.

Heat transfer coefficients for the finned tubes, on a square foot of area basis, are slightly less than those for the plain tube. This may be attributed to the increased thickness of the boundary layer in gas flows, and the establishment of dead zones in the corners of the fin configurations.

## SUMMARY

The principal purposes of this investigation were to identify the flow regimes occurring during the evaporation of refrigerants inside tubes and to study their heat transfer characteristics. The important regimes were found to be the nucleate boiling, annular flow, and mist flow regimes. A fourth regime, transition between annular flow and mist flow, was also investigated. Transition (corre-

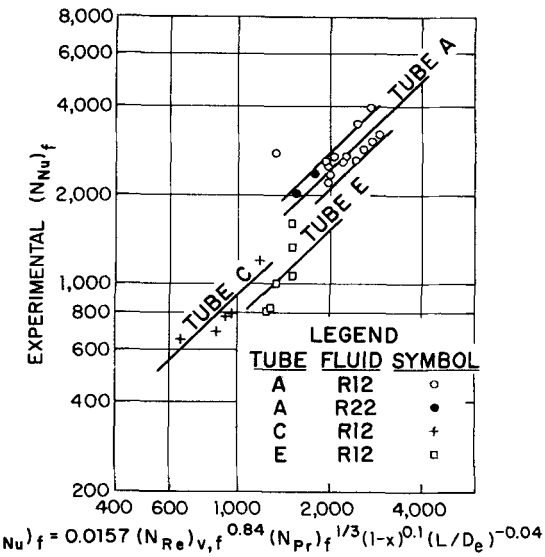


Fig. 15. Mist flow correlation for plain and finned tubes.

sponding to burnout or the dry wall condition) is normally considered to occur at a point; however, it appears that the transition takes place gradually and has the characteristics of an unstable regime.

Experimental heat transfer data obtained in the nucleate boiling regime were correlated by means of the McNelly correlation with modified coefficients. Tube orientation was found to be immaterial, and coefficients obtained in the internal fin tubes were higher than those predicted for plain tubes of the same equivalent diameter.

In the case of the annular flow regime, the experimental data obtained were not very well correlated by existing correlations, and a new correlation was developed. Heat transfer correlations for horizontal tubes were found to be higher than those for vertical tubes under similar conditions. Tube orientation did not appear to be important in the case of the finned tubes, and heat transfer coefficients fell between values for vertical and horizontal orientations in the plain tube.

Experimental data on conditions affecting the onset of the transition region were obtained and correlated. A strong relationship was found to exist between Weber number and vapor Reynolds number at transition. It was shown that transition was a boundary layer type of phenomenon and a method was developed for correlating transition data in tubes of varying size and shape. The vapor fraction at transition was found to be substantially independent of tube orientation. Transition was found to take place at lower vapor fractions in internal fin tubes than in plain tubes.

The heat transfer characteristics of the mist flow regime were found to be essentially those of a superheated vapor stream. A slight improvement over the superheated vapor coefficients was observed, and it was postulated that this was due to migration of liquid droplets to the wall, with subsequent flash evaporation. No effect of tube orientation was observed, and heat transfer coefficients for the two finned tubes studied were found to be lower than those for the plain tubes. Experimental heat transfer data were correlated by the Heineman correlation, modified to take into account the migrating droplet effect.


## ACKNOWLEDGMENT

The authors gratefully acknowledge the fellowship grant and the tubes provided by the Wolverine Tube Division of Calumet and Hecla, Inc.; the gift of Freon-12 and Freon-22 fluorocarbons by the E. I. du Pont deNemours and Company, Inc., and permission by the Computing Center of The University of Michigan to use the IBM-7090 digital computer to analyze the experimental data.


## NOTATION

$A$ = surface area, sq. ft.
$C$ = constants in equations
$c$ = specific heat at constant pressure, B.t.u./(lb.)(°F.)
$D_e$ = equivalent diameter (4 times mean hydraulic radius), ft.
$G$ = mass flow rate, lb./(hr.)(sq. ft.)
$g$ = acceleration due to force of gravity, (ft./hr.)/hr.
$g_c$ = gravitational acceleration constant, (ft./hr.)/hr.
$h$ = heat transfer coefficient, B.t.u./(hr.)(sq.ft.)(°F.)
$h_b$ = boiling heat transfer coefficient, B.t.u./(hr.)(sq. ft.)(°F.)
$h_l$ = heat transfer coefficient for liquid flowing alone in tube, B.t.u./(hr.)(sq. ft.)(°F.)
$h_{tp}$ = two-phase heat transfer coefficient, B.t.u./(hr.)(sq. ft.)(°F.)
$k$ = thermal conductivity, B.t.u./(hr.)(sq. ft.)(°F./ft.)
$L$ = tube length, ft.
$p$ = absolute pressure, lb.$_f$/sq. ft.
$Q$ = unit heat flux, B.t.u./(hr.)(sq. ft.)
$q$ = heat duty, B.t.u./hr.
$T_w$ = wall temperature, °F.
$T_{sat}$ = saturation temperature, °F.
$v$ = velocity, ft./sec.
$x$ = vapor fraction (by weight)

### Greek Letters

$\lambda$ = latent heat of vaporization, B.t.u./lb.
$\mu$ = viscosity, lb./ft./hr.
$\rho$ = density, lb./cu. ft.
$\sigma$ = surface tension, lb./ft.

### Subscripts

1,2,3,4,5,6 = constants in equations
$f$ = conditions referring to film
$l$ = conditions referring to liquid
$v$ = conditions referring to vapor
$w$ = conditions referring to wall temperature

### Superscripts

$a,b$ = constants used in correlating equations

### Dimensionless Groups

$N_{Fl}$ = flux number $= \dfrac{G\lambda}{Q}$
$N_{Nu}$ = Nusselt number, $\dfrac{hD}{k}$
$N_{Pr}$ = Prandtl number, $\dfrac{c\mu}{k}$
$(N_{Re})_l$ = Reynolds number for liquid flowing alone in tube
$(N_{Re})_v$ = Reynolds number for vapor flowing alone in tube
$(N'_{Re})_v$ = see Equation (15)
$N_{We}$ = Weber number, $\left[\dfrac{x^2 G \mu_l}{g_c \sigma \rho_v}\right] (N_{Re})_l^{0.125}$
$X_{tt}$ = Martinelli two-phase friction factor

## LITERATURE CITED


1. Hsu, Y. Y., and R. W. Graham, *Natl. Aeronaut. Space Admin. Tech. Note 1564* (1963).
2. Worsøe-Schmidt, P., *Ingeniøeren* (Danish), intern. ed., **3**, 84 (1960).
3. Sachs, P., and R. A. K. Long, *Intern. J. Heat Mass Transfer*, **2**, 222 (1960).
4. Dengler, C. E., and J. N. Addoms, *Chem. Eng. Progr. Symposium Ser. No. 18*, **52**, 95 (1956).
5. Guerrieri, S. A., and R. D. Talty, *ibid.*, 69.
6. Silvestri, M., *Am. Soc. Mech. Engrs. Paper* 39, Pt. II, 341 (1962).
7. Lavin, J. G., Sc. D. thesis, Univ. Michigan, Ann Arbor (1963).
8. Jakob, M., "Heat Transfer," Vols. I and II, Wiley, New York (1949, 1957).
9. Rounthwaite, C., and M. Clouston, *Am. Soc. Mech. Engrs. Paper* 23, Pt. I, 200 (1962).
10. McNelly, M. J., *J. Imp. Coll. Chem. Eng. Soc.*, **7**, 19 (1953).
11. Myers, J. E., and D. L. Katz, *Chem. Eng. Progr. Symposium Ser. No. 5*, **49**, 107 (1953).
12. Bennett, J. A. R., J. G. Collier, H. R. C. Pratt, and J. D. Thornton, *Trans. Inst. Chem. Engrs.*, **39**, 113 (1961); *AERE-R 3159* (1959).
13. Groothius, H., and W. P. Hendal, *Chem. Eng. Sci.*, **11**, 212 (1959).
14. Heineman, J. B., *ANL 6213* (1960).



*Manuscript submitted September 2, 1964; revision received June 14, 1965; paper accepted July 23, 1965. Paper presented at A.I.Ch.E. Memphis meeting.*